Journal of Soil Science and Plant Nutrition (2024) 24:732–748
https://doi.org/10.1007/s42729-023-01579-8

ORIGINAL PAPER

Transcriptome Analysis Reveals Candidate Genes Involved in Calcium Absorption of *Rosa roxburghii* Plants and their Effects on the Bioactive Substance Accumulation in Fruit

Zhao Wang[1,2] · Min Lu[1] · Huaming An[1]

Received: 31 July 2023 / Accepted: 6 December 2023 / Published online: 19 December 2023

Abstract

The objective of this research was to explore the candidate genes involved in calcium absorption of *R. roxburghii* plants, as well as their relationship with the bioactive substance accumulation in the fruit. RNA-seq and qRT-PCR were used to analyze the transcriptomic profiles of the roots and leaves of plants during calcium absorption. Based on the correlation between gene expression and calcium absorption rate, ion channels and carrier proteins were selected to further verify their response to exogenous calcium supplement and functions on the accumulation of ascorbate (AsA), flavonoid, and triterpenoid in the fruit. Transcriptome and qRT-PCR analysis revealed that a total of 25 candidate genes from seven families have been found to be closely associated with Ca^{2+} absorption, namely, *cyclic nucleotide-gated ion channel (CNGC)*, *zinc transporter (ZTP)*, *metal tolerance protein (MTP)*, *ER-type Ca^{2+} ATPase (ECA)*, *auto-inhibited Ca^{2+} ATPase (ACA)*, *glutamate receptor (GLR)*, and *natural resistance-associated macrophage protein (NRAMP)*. Among these, *RrCNGC1/7/10/12* and *RrMTP2* play a vital role in responding to changes in external calcium levels. Moreover, exogenous Ca^{2+} promoted the accumulation of bioactive compounds such as AsA, total flavonoid, and total triterpenoid in fruits. *RrCNGC2/3/12*, *RrZTP1*, and *RrGLR1* significantly responded to exogenous Ca^{2+} supplement, of which *RrCNGC12* positively correlating with the levels of the above three types of bioactive substances. Seven families of ion channels and carrier proteins were jointly involved in calcium absorption and homeostasis in *R. roxburghii* plants, and *RrCNGC12* play a critical role in the calcium-mediated regulation of fruit quality formation.

Keywords *Rosa roxburghii* · Calcium · Uptake and transport · RNA-Seq · Fruit quality

1 Introduction

Calcium (Ca^{2+}) is an essential nutrient for plant growth and a second messenger in plants. The cytosolic concentration of Ca^{2+} ($[Ca^{2+}]_{cyt}$) significantly influences crop growth and development (Hirschi 2004). Various environmental stimuli can cause changes of $[Ca^{2+}]_{cyt}$, and the increase of free Ca^{2+} in cellular is an early and crucial event of plant defense signaling (Lecourieux et al. 2006). Studies have shown that Ca^{2+} can promote the synthesis of multiple secondary metabolites by transmitting secondary signals to downstream target enzymes and thus enhances plant resistance to adverse external environments (Zhao et al. 2005; Ahmad et al. 2016; Martins et al. 2021; Michailidis et al. 2019; Juric et al. 2020). For example, melatonin induces the production of phenolic compounds by causing the influx of extracellular Ca^{2+} into cells and activating Ca^{2+}/calmodulin (CaM) signaling (Vafadar et al. 2020). Under cold stress, Ca^{2+} strengthen the cold

Highlights
- We conducted experiments using *Rosa roxburghii* saplings as materials in three stages: Ca^{2+} starvation, rapid Ca^{2+} uptake, and Ca^{2+} saturation.
- We investigated the Ca^{2+} uptake patterns and molecular mechanisms in *Rosa roxburghii* plants.
- Some genes associated with Ca^{2+} uptake have an impact on fruit bioactive substance accumulation.

✉ Huaming An
hman@gzu.edu.cn

[1] Guizhou Engineering Research Center for Fruit Crops, Agricultural College, Guizhou University, Guiyang 550025, People's Republic of China

[2] South Subtropical Crops Research Institute CATAS, Chinese Academy of Tropical Agricultural Sciences, Zhanjiang 524000, People's Republic of China

resistance of plant by maintaining soluble sugar and protein content in cells and increasing the content of unsaturated fatty acid in membrane (Shi et al. 2017). Wang et al. (2022) discovered that *CaM* and calmodulin-like (*CML*) genes contribute to improving drought resistance in maize. Therefore, the level of Ca^{2+} in the cytoplasm and the combination of Ca^{2+} sensors and downstream proteins participate in the growth and development process of plants.

Plant signals and responses are related to variations in $[Ca^{2+}]_{cyt}$, which is tightly regulated by a network of channels and carriers responsible for Ca^{2+} homeostasis and the production of Ca^{2+} signals (Tang and Luan 2017). These carriers and channels include passive fluxes (Ca^{2+} channels) and active transport (Ca^{2+}-ATPases and Ca^{2+}-antiporters) across the plasma membrane or endomembranes (Sanders et al. 1999, 2002; Demidchik et al. 2018; Zhang et al. 2019). A variety of Ca^{2+} channels have been found in plant cell membranes, primarily divided into three categories: depolarization-activated Ca^{2+}-permeable channels (DACCs) and hyperpolarization-activated Ca^{2+}-permeable channels (HACCs), and nonselective cation channels (NSCCs). Among these, HACCs in root hairs are highly selective for Ca^{2+} (Véry and Davies 2000), although some studies suggest that plant Ca^{2+} conductances are primarily mediated by NSCCs (Liu et al. 2018). These ion channels are closely related to the production of calcium signals and response to abiotic stress. Gao et al. (2016) reported that R491Q or R578K point mutations in cyclic nucleotide-gated channel 18 (CNGC18) resulted in abnormal Ca^{2+} gradients and defects in pollen tube guidance by impairing the activity of CNGC18 in *Arabidopsis*. The upregulation of Ca^{2+} influx channel protein mid1-complementing activity 1 (*MCA1*) gene and the downregulation of efflux channel protein cation exchanger 1 (*CAX*) and autoinhibited Ca^{2+}-ATPase 1 (*ACA1*) genes in the cytoplasmic membrane jointly facilitated the increase of Ca^{2+} in the cytoplasm (Yang et al. 2022). In conclusion, channels and carriers of calcium ions and other cations jointly mediate the transport of Ca^{2+}.

Rosa roxburghii Tratt. is a perennial shrub of the Rosaceae family, which is widely distributed in the karst region of southwest China with calcium-rich soil. The fruits of this species are valued for their nutritional and medicinal characteristics, especially their high ascorbic acid (AsA), triterpenoid, and flavonoid levels, and therefore believed to have valuable senescence-retarding and cancer-preventing effects (Ojo et al. 2022). Various studies have shown that Ca^{2+} plays a vital regulatory role in the growth and the formation of quality of *R. roxburghii* fruits (Luo et al. 2004). Increasing exogenous Ca^{2+} can induce the expression of *GalLDH* and *GPP* genes involved in the AsA synthesis pathway, as well as *DHAR* and *MDHAR* genes involved in the AsA regeneration pathway (Li and An 2016). This process promotes the synthesis and accumulation of AsA in *R. roxburghii* fruits (Zhang et al. 2012). Ca^{2+} needs to rely on the coordinated transport of ion channels and carriers to function, but the absorption and transport mechanism of Ca^{2+} in *R. roxburghii* have not been thoroughly studied. In this study, we analyzed the transcriptome characteristics during calcium absorption in *R. roxburghii* cv. 'guinong 5' using RNA-Seq technology and screened for candidate carrier or channel protein related to calcium absorption. And we also explored their possible relationship with the accumulation of main bioactive substances (AsA, flavonoids, and triterpenoids) in fruits. The results of this experiment have provided valuable candidate genes to help understand the calcium absorption mechanism of *R. roxburghii* and explored its relationship with the accumulation of bioactive substances.

2 Material and Methods

2.1 Material Selection and Cultivation

The *R. roxburghii* cv. 'guinong 5' saplings propagated from cuttings were planted in *R. roxburghii* resource nursery of Guizhou University. Saplings with 3-month age which showed similar growth and size were selected and transferred to a 1/8 concentration of Hoagland and Aron nutrient solution from soil for pre-cultivation. The nutrient solution was changed every 3 days, and its pH value was adjusted to 6.5 using 0.1 mol L^{-1} H_2SO_4 or NaOH. The culture temperature was maintained at 20 ℃.

2.2 *Determination of Different Periods of Ca^{2+} Uptake in R. roxburghii Plants*

Yang and Fan (2022) found that the growth of *R. roxburghii* plants was most optimal at the Ca^{2+} concentration of 50–100 mg L^{-1}. After conducting pre-experiments (Fig. S1), we selected the Ca^{2+} concentration of 2 mmol L^{-1} for the uptake experiment. The saplings were starved in deionized water for 24 h after being pre-cultured for 2 months. Following this, they were transferred to an culture solution consisting of 2 mmol L^{-1} $Ca(CH_3COO)_2$. Two time intervals, either every 1 h or every 10 min, were used to change the culture solution and determine the concentration of Ca^{2+} in the culture solution. This was conducted to determine the rapid Ca^{2+} uptake period and Ca^{2+} saturation period of the saplings. The uptake rate (μg g^{-1} h^{-1}) was calculated using the equation: reduced Ca^{2+} concentration (μg mL^{-1}) × total volume of nutrient solution (mL) / (fresh root weight (g) × time (h)).

2.3 Transcriptome Sequencing Analysis

2.3.1 Sampling and RNA Extraction

At the Ca^{2+} starvation, rapid Ca^{2+} uptake, and Ca^{2+} saturation stages, white aquatic roots and leaves of *R. roxburghii* saplings were collected separately to extract total RNA for transcriptome sequencing and qRT-PCR. Three biological replicates were used. The collected samples were stored at – 80 °C after being treated with liquid nitrogen for the extraction of total RNA. Each RNA sample was divided into two aliquots: one for RNA-seq and the other for qRT-PCR.

2.3.2 Sequencing and Quality Control

mRNA was purified from total RNA using poly-T oligo-attached magnetic beads. Fragmentation was carried out using divalent cations under elevated temperature in NEBNext First Strand Synthesis Reaction Buffer (5X). First-strand cDNA was synthesized using random hexamer primer and M-MuLV Reverse Transcriptase. Second-strand cDNA synthesis was subsequently performed using DNA Polymerase I and RNase H. The library fragments were purified with AMPure XP system (Beckman Coulter, Beverly, USA). Then 3 µl USER Enzyme (NEB, USA) was used with size-selected, adaptor-ligated cDNA at 37 °C for 15 min followed by 5 min at 95 °C before PCR. Then PCR was performed with Phusion High-Fidelity DNA polymerase, Universal PCR primers and Index (X) Primer. At last, PCR products were purified (AMPure XP system) and library quality was assessed on the Agilent Bioanalyzer 2100 system. The clustering of the index-coded samples was performed on a cBot Cluster Generation System using TruSeq PE Cluster Kit v4-cBot-HS (Illumia) according to the manufacturer's instructions. After cluster generation, the library preparations were sequenced on an Illumina platform and paired-end reads were generated.

The raw reads were further processed with a bioinformatic pipeline tool, BMKCloud (www.biocloud.net) online platform. Raw reads of fastq format were firstly processed through fastp 0.21.0 (Chen et al. 2018). In this step, clean reads were obtained by removing reads containing adapter, reads containing ploy-N, and low-quality reads from raw data. At the same time, Q20, Q30, GC-content, and sequence duplication level of the clean data were calculated. All the downstream analyses were based on clean data with high quality. These clean reads were then mapped to the reference genome sequence. Hisat2 (Kim et al. 2015) tools soft were used to map with reference genome. Using StringTie (Pertea et al. 2015) to assemble reads been compared.

2.3.3 Gene Functional Annotation

Gene function was annotated using DIAMOND (Buchfink et al. 2015) based on the following databases: Nr (NCBI non-redundant protein sequences) (Deng et al. 2006); Pfam (Protein family) (Finn et al. 2014); KOG/COG (Clusters of Orthologous Groups of proteins) (Tatusov et al. 2000; Koonin et al. 2004); Swiss-Prot (A manually annotated and reviewed protein sequence database) (Apweiler et al. 2004); KO (KEGG Ortholog database) (Kanehisa et al. 2004); GO (Gene Ontology) (Ashburner et al. 2000).

2.3.4 Screening of Differentially Expressed Genes (DEGs) and Its GO and KEGG Enrichment Analysis

FPKM (fragments per kilobase of transcript per million fragments mapped) was used as a measure of transcript or gene expression level. DESeq2 software was used to perform differential gene expression analysis (Love et al. 2014), with DEGs screened based on the criteria of fold change ≥ 1.2 and FDR < 0.01. FDR was obtained by correcting the difference significance *p*-value. DEGs were annotated to the GO database, and their functional distribution statistics were counted, analyzed, and plotted (Young et al. 2010). The DEGs were also compared with the KEGG database to investigate the metabolic pathways and signaling pathways in which they are involved (Kanehisa et al. 2008).

2.4 R. roxburghii Saplings Treated with Different Levels of Calcium Supply

The 1/8 concentration of Hoagland and Arnon formula was used as the basic nutrient solution in the experiment, with slight modifications made to remove all Ca^{2+}-containing components and to equalize nitrogen differences with 40 mg L^{-1} NH_4NO_3, while keeping other element concentrations unchanged. Calcium concentrations were controlled through $Ca(CH_3COO)_2$. According to the research of Yang and Fan (2022), we designed three calcium concentration treatments, namely 0 mmol L^{-1}, 0.5 mmol L^{-1}, and 2 mmol L^{-1}. The pH of nutrient solution were adjusted to 6.5 using 0.1 mol L^{-1} NaOH and H_2SO_4. The cultivation temperature was 20 °C. *R. roxburghii* saplings were starved for 24 h and then transferred to the three nutrient solutions. Hydroponic roots and leaves of saplings in different treatments were collected after 0 day, 1 day, and 7 days of cultivation, respectively. A portion is dried to constant weight and stored at ordinary temperature, while another portion is treated with liquid nitrogen and stored at – 80 °C. The calcium content and the expression

of candidate genes in these samples were determined. Each treatment was replicated biologically three times.

2.5 The Spatiotemporal Expressive Specificity of Candidate Genes

Excellent perennial asexual lines of *R. roxburghii* cv. 'guinong 5' were selected as test materials. Fruits, petals, and leaves from the upper and middle portions of the crown at 30 days after anthesis were used as samples for analyzing of the expression patterns in various organs. Fruit samples were taken at 30, 60, and 90 days after anthesis, at 10 am, with at least 300 g of fruits collected each time. The expression of candidate genes was determined using qRT-PCR in different developmental stages of fruits and in different tissue samples.

2.6 *Spraying Plant Crown* In Vivo *with Exogenous* Ca^{2+}

Good asexual lines of perennial *R. roxburghii* were sprayed with Ca^{2+} solution on the plant crown at 20 days, 50 days, and 80 days after anthesis. Thirty fruits were sampled at 30 days (30 May), 60 days (30 June), and 90 days (30 July) after anthesis. A portion is dried to constant weight and stored at ordinary temperature, while another portion is treated with liquid nitrogen and stored at − 80 °C. We set up four concentration treatments by $Ca(CH_3COO)_2$ solution, namely 100 mg L^{-1}, 300 mg L^{-1}, 500 mg L^{-1}, and 700 mg L^{-1}, with clear water as the control (Luo et al. 2004), and five trees grown in each treatment. The content of calcium, AsA, total flavonoid, and total triterpenoid content, as well as the expression of candidate genes, were determined in the samples from different treatments. Three biological replicates were analyzed for each indicator.

2.7 *Soaking Fruit* In Vitro *with Exogenous* Ca^{2+}

The *R. roxburghii* fruits of uniform development were collected in late July. According to the method of Zhang et al. (2012), each fruit was divided into three portions and placed in a culture solution with the following formulation: 2 mmol L^{-1} $CaSO_4$ + 15 mmol L^{-1} glucose, 2 mmol L^{-1} $CaSO_4$ + 15 mmol L^{-1} glucose + 5 mmol L^{-1} EGTA, and 15 mmol L^{-1} glucose as a control. Samples were taken after incubation in a light incubator for 0, 3, 6, 12, and 24 h, during which 54 μmol m^{-2} s^{-1} of light was provided from 8:00 to 19:00 at 25 ℃, with three biological replicates. The samples were taken to determine the content of calcium, AsA, total flavonoid, and total triterpenoid, as well as the expression of candidate genes, and the determination was repeated three times.

2.8 Measurement of Calcium, AsA, Total Flavonoid, and Total Triterpenoid

2.8.1 Determination of Calcium Content

The calcium content was determined by the HNO_3-$HClO_4$ digestion method and inductively coupled plasma emission spectrometry (ICP-AES). The samples were baked at 110 °C for 0.5 h and then placed in a thermostat at 70 °C until their weight became constant. The dried samples were ground and passed through a 100 mesh nylon sieve. The sample was weighed 0.5 g, incubated overnight in 15 mL of mixed acid (HNO_3/$HClO_4$ = 9:1, v/v), heated on an electric hot plate until white smoke was emitted, and continued to heat until about 1 mL of digest remained. After cooling, the digest was transferred to a clean volumetric flask, fixed to 50 mL, filtered, and the calcium content was determined by ICPE-9800 inductively coupled plasma emission spectrometer. Element content (mg g^{-1}) was calculated as $(D-B)\times V/(W\times 1000)$, where D is the detection value of the sample element concentration (mg L^{-1}), B is the blank detection value (mg L^{-1}), V is the total volume of the sample after digestion (mL), and W is the sample weight (g). All tests were performed in three biological and technical replicates.

2.8.2 Determination of AsA Content

Liquid chromatography was used for the determination of AsA content (Wang and An 2013). The tissue samples were ground evenly with 5 mL of 6% metaphosphoric acid solution in a pre-chilled mortar. The solution was then transferred to a 10-mL centrifuge tube and centrifuged for 15 min at 4 °C and 10,000 r/min. The supernatant was removed to a 10-mL centrifuge tube, and 3–4 mL of extract was added to the remaining residue, which was then centrifuged for an additional 10 min under the same conditions. The supernatant was removed and combined, and the volume was made constant to 10 mL. This solution was passed through a 0.45-μm filter membrane to obtain the AsA extract for determination. The AsA content was determined by high-performance liquid chromatography (HPLC) under the following conditions: Wondasil C18 column (4.6 mm × 150 mm, 5 μm); mobile phase, 0.2% metaphosphoric acid solution; flow rate, 1 mL/min; column temperature, 30 ℃; UV detector, 254 nm; injection volume, 20 μL. The AsA content was calculated based on the peak value of the HPLC spectrum (Fig. S2) using the following formula: AsA content (mg/100 g) = $(m_1\times v_2\times 10^{-6}\times 100)/(m\times v_1)$, where m is the mass of the sample weighed in grams; m_1 is the mass of AsA in the solution to be measured (g), calculated using the standard curve; v_1 is the volume of the extraction solution used for determination in the sample (mL); and v_2 is the total volume of the sample presented (mL).

2.8.3 Determination of Total Triterpenoid Content

A standard curve was prepared using ursolic acid as the standard. The tissue sample weighing 0.5 g was added to 8 mL of 75% ethanol solution, then centrifuged at 7000 r/min for 10 min, after 50 min of ultrasonic extraction at 50 ℃. The supernatant was aspirated and fixed to a volume of 10 mL, after which it was shaken well. For determination, 0.2 mL of the extract was taken, and 0.5 mL of 5% vanillin-acetic acid solution and 0.8 mL of perchloric acid were added. The resulting mixture was shaken well and heated in a water bath at 60 ℃ for 20 min, and then immediately cooled in ice water. Finally, 3.5 mL of glacial acetic acid was added, shaken well and the absorbance was measured at a wavelength of 545 nm. The total triterpenoid content was calculated using the following formula: total triterpenoid content (mg/100 g) = $(m_1 \times v_2 \times 10^{-6} \times 100)/ (m \times v_1)$, where m is the mass of the sample weighed in grams; m_1 is the mass of total triterpenoid in the solution to be measured (g), calculated using the standard curve; v_1 is the volume of the extraction solution used for determination in the sample (mL); and v_2 is the total volume of the sample presented (mL).

2.8.4 Determination of Total Flavonoid Content

The $NaNO_2$-$Al(NO_3)_3$ colorimetric method was employed to determine the total flavonoid content. The rutin standard was used to prepare the standard curve. 0.5 g of the sample was weighed and sonicated for 2 h in 15 mL of 30% methanol. The mixture was then centrifuged at 8000 r/min for 10 min, and the supernatant was extracted. The extracted supernatant was fixed to a volume of 10 mL, after which 2 mL of the extract was pipetted into a 10-mL centrifuge tube. To this solution, 0.4 mL of 5% $NaNO_2$, 0.6 mL of 10% Al $(NO_3)_3$, and 4 mL of 4% NaOH were added. The resulting mixture was shaken well at each step, left at ordinary temperature for 6 min, fixed to a volume of 10 mL with 30% methanol, and left standing for 15 min. The absorbance value at 510 nm was measured, and each sample was replicated three times. The total flavonoid content was calculated using the following formula: total flavonoid content (mg/100 g) = $(m_1 \times v_2 \times 10^{-6} \times 100)/ (m \times v_1)$, where m is the mass of the sample weighed (g); m_1 is the mass of total flavonoid in the solution measured (g) using the standard curve; v_1 is the volume of the extraction solution used for the determination in the sample (mL); and v_2 is the total volume of the sample presented (mL).

2.9 RNA Extraction and qRT-PCR

Total RNA was extracted using the Tiangen RNAprep Pure Polysaccharide Polyphenol Plant Total RNA Extraction Kit based on the manufacturer's instructions. The RNA was reverse transcribed using the RNA PCR Kit Ver. 2.1 (TaKaRa, Dalian, China). Primers were synthesized according to Table S1, and qRT-PCR was performed using TB Green Premix Ex Taq II (Tli RNaseH Plus) (Code No. RR820A/B). Ct values were calculated based on three replicate technical experiments performed on three biological replicates. The *UBQ* gene was used as an internal reference gene for normalization. The relative expression levels of target genes were determined using the $2^{-\Delta\Delta Ct}$ method.

2.10 Statistical Analysis

Data were processed and plotted using Excel 2016 data processing software. Heat maps were plotted using TBtools, and correlation and significance of differences were analyzed using SPSS 18.0. Data were presented as mean values ± SEs, and statistical analyses were performed using the Duncan test ($p < 0.05$).

3 Results

3.1 *Determination of Different Periods of Ca^{2+} Uptake in R. roxburghii*

In this experiment, a 2 mmol L^{-1} $Ca(CH_3COO)_2$ solution was used as the absorption solution and the Ca^{2+} absorption characteristic of *R. roxburghii* at different times was analyzed (Fig. 1). Calcium content in absorption solution had the most reduction within the first hour of absorption. The calcium saturation was reached after 5–6 h. Next, we conducted experiments at 10-min intervals, and the rapid Ca^{2+} uptake period of *R. roxburghii* occurred within 0–10 min. Therefore, we chose 5 min as the rapid Ca^{2+} uptake period, 6 h as the Ca^{2+} saturation period, and 0 min as the starvation period.

3.2 Quality Assessment of Transcriptome Sequencing and Gene Annotation

The main site of Ca^{2+} uptake in plants is the root, driven by transpiration pull. Accordingly, the transcriptome of *R. roxburghii* roots and leaves was sequenced at different calcium uptake periods (0 min, 5 min, and 6 h). After quality control, a total of 116.13 Gb of clean data were obtained. Each sample's clean data reached 5.71 Gb, Q30 was 94.06% and above, and the GC content ranged from 46.24 to 48.34% (Table S2). The check of base type distribution showed stable content of GC and AT (Fig. S3), and the sequencing error rate was below 0.0005 (Fig. S4). The results of sample replication test demonstrated good sample reproducibility (Fig. 2A). Referring to the selected reference genome

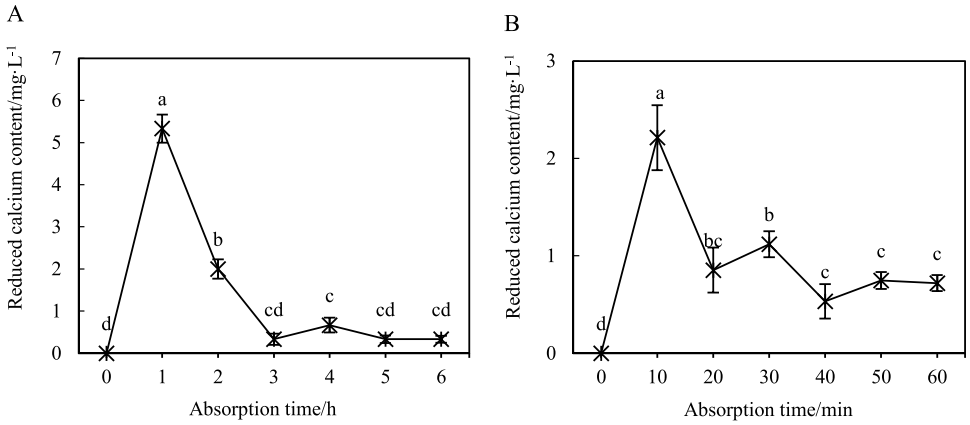

Fig. 1 Calcium absorption dynamics of *R. roxburghii*. Note: **A** Hourly calcium absorption dynamics of *R. roxburghii*; **B** Calcium absorption dynamics of *R. roxburghii* every 10 min. There are significant time differences between letters

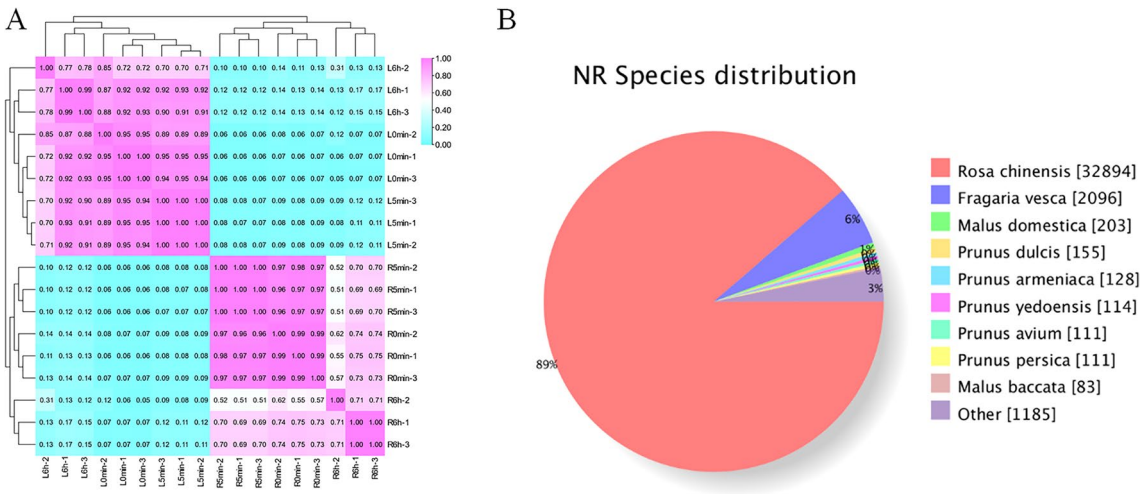

Fig. 2 Sample repeatability test (**A**) and distribution statistics of different species in NR notes (**B**). Note: **A** The values in the figure represent the correlation between samples; coordinate name is tissue (L/R) + treatment time (0 min/5 min/6 h) + duplicate number, L for leaf, R for root

sequences, the number of annotated unigene was 37,241, and 86.1% of unigene was compared to the NR database (Table S3). Statistical analysis of the annotation results from NR database revealed (Fig. 2B) that *R. roxburghii* has a closer relationship with *Rosa chinensis*, followed by *Fragaria vesca*.

3.3 Identification of DEGs and Their GO and KEGG Enrichment

Using the screening criteria of fold change ≥ 1.2 and FDR < 0.01, a total of 12,314 DEGs were identified in the experiment. Of these, 1323 genes in roots and 1546 genes in leaves were upregulated in expression during the rapid Ca^{2+} uptake period compared to the starvation period. The comparison between groups demonstrated more DEGs in roots than in leaves (Fig. S5), suggesting a more active response in roots during Ca^{2+} uptake. GO functional enrichment contained three main branches (Fig. 3A), including biological process, molecular function, and cellular component. DEGs were mostly involved in cellular processes and metabolic processes within the biological process module, membrane and membrane part within the cellular component module, and catalytic activity, binding, and transporter activity within the molecular function module. The KEGG pathway classification grouped all DEGs into five major categories, with a total of 134 pathways (Fig. 3B). The DEGs of MAPK signaling pathway, plant hormone signal transduction, and plant-pathogen interaction accounted for a higher percentage, up to 5.61%, 7.61%, and 11.05%, respectively. This finding demonstrates that Ca^{2+} is involved in signal transduction, multiple metabolic processes, and defense processes in *R. roxburghii*.

3.4 Identification and Expression Validation of Genes Involved in Calcium Uptake and Transport in R. roxburghii

Based on previous research literature, we screened the DEGs of ion channels and carrier that were related to ion transport, combined with the results of GO annotation, COG function enrichment, and KEGG pathway enrichment. We further correlated these findings with the changes in the Ca^{2+} uptake rate of *R. roxburghii* saplings (Table 1). We used the screening criteria of correlation coefficient absolute value > 0.7 and FPKM values > 10 to identify candidate genes involved in calcium uptake and transport. By these methods, we screened 25 candidate genes in leaves and roots (Fig. 4). These genes belong to seven gene families, which include the cyclic nucleotide-gated ion channel (*CNGC*), zinc transporter (*ZTP*), metal tolerance protein (*MTP*), ER-type Ca^{2+} ATPase (*ECA*), Autoinhibited Ca^{2+} ATPase (*ACA*), glutamate receptor (*GLR*), and natural resistance-associated macrophage protein (*NRAMP*). The expression of *RrACA1/2/3*, *RrCNGC1/2/3/4/5/6/7/8*, *RrECA1*, *RrGLR1*, and *RrMTP1/2* in leaves was positively correlated with the rate of Ca^{2+} uptake. This indicates that they facilitate the upward transport of Ca^{2+} and promote its uptake. In the root, the expression of *RrCNGC9/10*, *RrECA2*, and *RrGLR2* was positively correlated with the rate of Ca^{2+} uptake, suggesting that these genes play a positive regulatory role in Ca^{2+} uptake. Interestingly, we found that the expression of genes *RrCNGC11/12*, *RrMTP1/3*, *RrNRAMP1*, and *RrZTP1/2* in roots exhibited a negative correlation with the rate of Ca^{2+} uptake, suggesting that these genes may regulate ion homeostasis during starvation and calcium saturation periods. qRT-PCR results confirmed the reliability of the transcriptome sequencing results (Figs. S6 and S7).

3.5 *Changes of Calcium Content in R. roxburghii Under Different Calcium Concentrations and the Response of Genes Related to Ca^{2+} Uptake and Transport*

To further identify genes that respond to different levels of calcium, the calcium content of roots and leaves was measured under different calcium concentrations (0 mmol L^{-1}, 0.5 mmol L^{-1}, and 2 mmol L^{-1}), and the expression of 25 candidate genes was assessed in this experiment (Fig. 5). The results revealed that the calcium content in leaves and roots increased rapidly after 0.5 mmol L^{-1} and 2 mmol L^{-1} Ca^{2+} treatments from 0 to 1 day compared with the control (0 mmol L^{-1} Ca^{2+}). After that, the calcium content in roots kept increasing, while the calcium content in leaves showed a slight decreasing trend, indicating that calcium migrated from leaves to roots in the later stages of calcium uptake. The qRT-PCR analysis and correlation analysis indicated that the expression of *RrCNGC7* in the roots was significantly and positively correlated with the calcium content, while the expression of *RrCNGC1/10/12* and *RrMTP2* in leaves was significantly and positively correlated with the calcium content. When the external calcium concentration changes, these genes played a key role in calcium accumulation within roots or leaves.

3.6 Spatiotemporal Expression Characteristics of Candidate Genes

In this experiment, the expression patterns of 25 candidate genes were assessed in various tissues of *R. roxburghii*, including fruits at 30 days after anthesis, leaves, and petals, as well as in fruits at different developmental stages (30, 60, and 90 days after anthesis). The results demonstrated that the expression of these genes was tissue-specific and time-specific (Fig. 6). The expression levels of most genes were significantly higher in leaves and fruits than in petals, and they were also higher in the later stages of fruit development compared to the early stages.

3.7 Relationship Between Calcium Uptake and Transport Genes and Major Active Substances in R. roxburghii Fruits

The *R. roxburghii* has a significant advantage compared to other plants in active substances of fruit, namely AsA, triterpenoid, and flavonoid. In Fig. 6, it was observed that the majority of candidate genes exhibited high expression levels in middle and late stage fruits. Consequently, the question arises: does Ca^{2+} regulate the synthesis of these substances? To seek answers, we conducted two treatments on *R. roxburghii*, namely exogenous Ca^{2+} soaking of friuts in vitro and spraying plant crown in vivo.

Using the common extracellular Ca^{2+} chelator, ethylenebis (oxyethylenenitrilo) tetraacetic acid (EGTA) to soak fruit, we observed that the treatment of Ca^{2+} add to glucose significantly increased the calcium content of the fruits, while the inclusion of EGTA led to a decrease in calcium levels. The trends of AsA, total triterpenoid, and total flavonoid were consistent with the trends observed for calcium content. After the treatment of spraying $Ca(CH_3COO)_2$ at concentrations ranging from 100 to 700 mg L^{-1}, it was observed that Ca^{2+} promoted the accumulation of the three active substances in the fruits at 30 and 60 days after anthesis. However, the optimal Ca^{2+} concentration for accumulation of these three substances was different at 90 days after anthesis, suggesting a dosage effect of calcium ions on these substances (Fig. 7).

Our correlation analyses and gene expression patterns revealed that the calcium content in fruits was significantly and positively correlated with the content of AsA, total

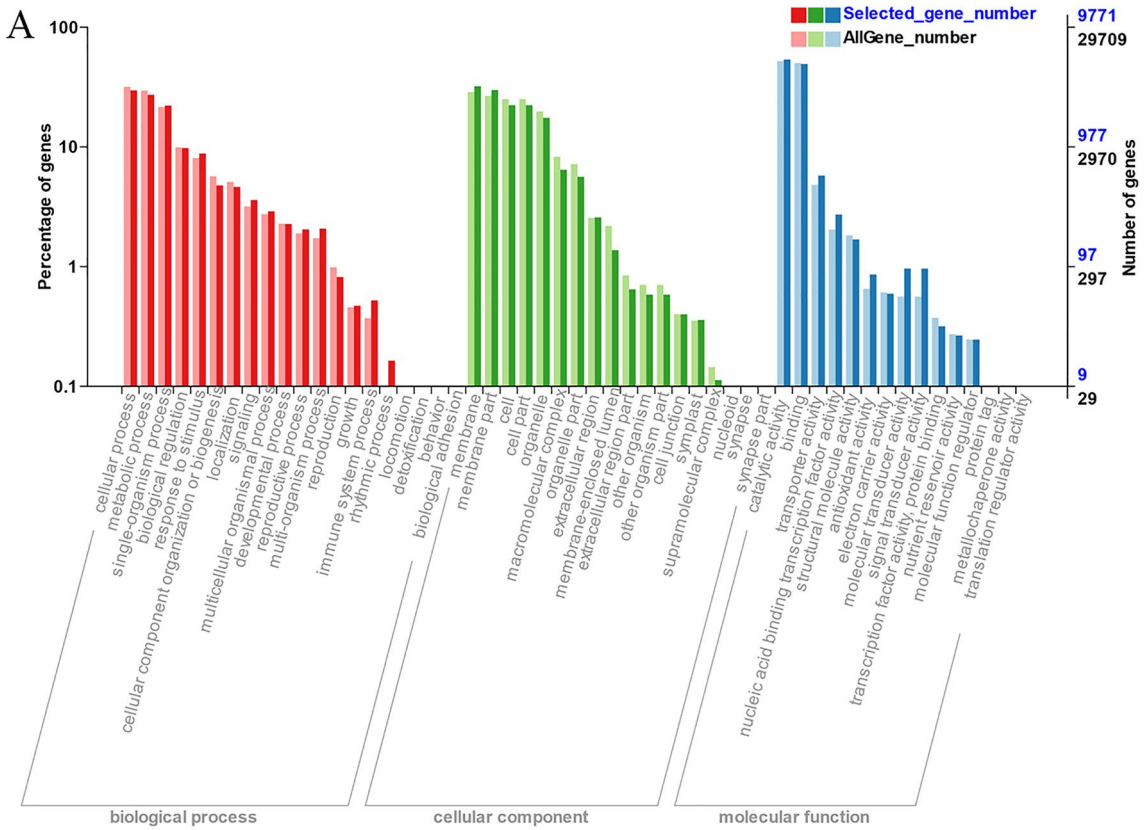
A
Selected_gene_number
AllGene_number
9771
29709
977
2970
97
297
9
29
Percentage of genes
Number of genes
100
10
1
0.1
cellular process
metabolic process
single-organism process
biological regulation
response to stimulus
cellular component organization or biogenesis
localization
signaling
multicellular organismal process
developmental process
reproductive process
multi-organism process
reproduction
growth
immune system process
rhythmic process
locomotion
detoxification
biological adhesion
behavior
membrane
membrane part
cell
cell part
organelle
macromolecular complex
organelle part
extracellular region
membrane-enclosed lumen
extracellular region part
other organism
other organism part
cell junction
symplast
supramolecular complex
nucleoid
synapse
synapse part
catalytic activity
binding
transporter activity
nucleic acid binding transcription factor activity
structural molecule activity
antioxidant activity
electron carrier activity
molecular transducer activity
signal transducer activity
transcription factor activity, protein binding
nutrient reservoir activity
molecular function regulator
protein tag
metallochaperone activity
translation regulator activity
biological process
cellular component
molecular function

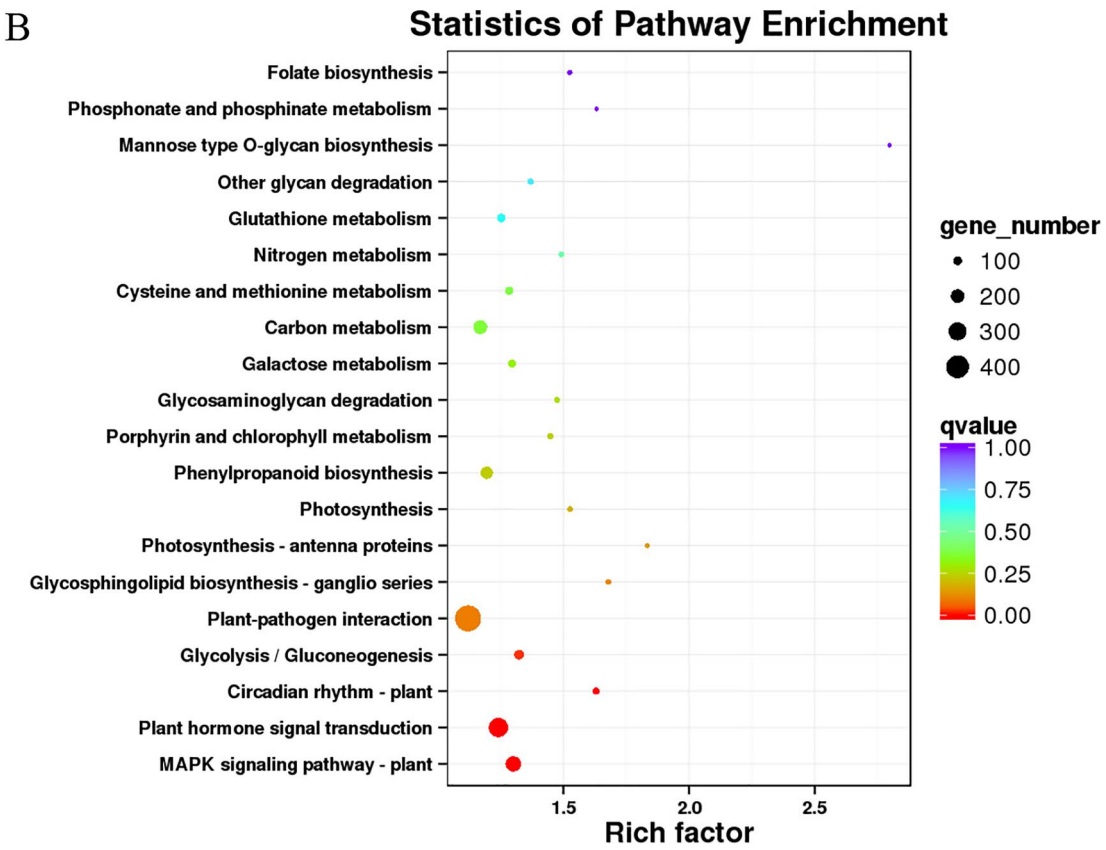
B
Statistics of Pathway Enrichment
Folate biosynthesis
Phosphonate and phosphinate metabolism
Mannose type O-glycan biosynthesis
Other glycan degradation
Glutathione metabolism
Nitrogen metabolism
Cysteine and methionine metabolism
Carbon metabolism
Galactose metabolism
Glycosaminoglycan degradation
Porphyrin and chlorophyll metabolism
Phenylpropanoid biosynthesis
Photosynthesis
Photosynthesis - antenna proteins
Glycosphingolipid biosynthesis - ganglio series
Plant-pathogen interaction
Glycolysis / Gluconeogenesis
Circadian rhythm - plant
Plant hormone signal transduction
MAPK signaling pathway - plant
1.5
2.0
2.5
Rich factor
gene_number
100
200
300
400
qvalue
1.00
0.75
0.50
0.25
0.00

◂**Fig. 3** DEG enrichment analysis. **A** Statistical diagram of GO annotation classification of DEG; **B** enrichment map of DEG KEGG pathway. Note: **A** The abscissa is the go classification, the left side of the ordinate is the percentage of the number of genes, and the right side is the number of genes; **B** the ordinate is the name of KEGG channel; the abscissa is the enrichment factor, representing the significance of DEG enrichment level in this pathway; the color of the circle represents *Q* value. The smaller this value is, the more reliable the enrichment significance of DEG in this pathway is; the size of the circle indicates the number of genes enriched in the pathway. The larger the circle, the more DEG

triterpenoid, and total flavonoid after the treatment of Ca^{2+} soaking fruits in vitro. And *RrCNGC3/12* and *RrGLR1* played a crucial role in this process (Fig. 8). The correlation coefficient between calcium content and the content of total triterpenoid and total flavonoid in the fruits was greater than 0.8 and showed a highly significant positive correlation with AsA after the Ca^{2+} spraying (Fig. 9). The expression of *RrCNGC2* and AsA content showed a highly significant positive correlation, and *RrCNGC12* was significantly correlated with the total triterpenoid and total flavonoid contents and clustered into one group at 30 days after anthesis. The correlation coefficients of calcium content with AsA and total triterpenoid in fruits at 60 days after anthesis were high, and the expression of *RrZTP1* was significantly and positively correlated with total flavonoid content. However, as the fruit develops, the correlation coefficients between calcium content in the fruits and the three substances gradually decreased, indicating that Ca^{2+} mainly regulates the formation of these substances in the early and middle stages of fruit development.

4 Discussion

4.1 The Uptake of Calcium by R. roxburghii Is a Rapid Process That May Be Involved in Plant Defense Against Pathogens

Compared to other plants, *R. roxburghii* has the highest content of AsA and is rich in flavonoids, triterpenoids, and other active substances. It grows in karst regions, where the soil calcium content is considerably high. Ca^{2+} uptake, transport, and function have been a hot topic of research in the field of plant nutrition. However, the calcium nutrition study of *R. roxburghii* is the early stages of physiological research.

In this experiment, we tried to explore the calcium absorption and transport mechanisms in *R. roxburghii*. Transcriptome sequencing is a common tool for molecular biology research now, with RNA-Seq being preferentially applied due to its high throughput, broad detection range, and accurate quantification (Bräutigam and Gowik 2010). To select suitable sequencing materials, we performed Ca^{2+} uptake tests in *R. roxburghii*. Our results revealed that the rapid uptake period occurred within 0–10 min, and the Ca^{2+} saturation state was reached after 5–6 h. Similarly, the fastest period of nutrient uptake for iron, phosphorus, potassium, and calcium was 1 h, after which the uptake rate decreased gradually until stabilization in *Malus hupehensis* (Fan and Yang 2014). Additionally, phosphorus-deficient maize plants sprayed with 200 mmol/L KH_2PO_4 showed that phosphorus was primarily absorbed within the first 6 h (Görlach et al. 2021), indicating that nutrient uptake is a rapid process.

Calmodulin (CaM) and calmodulin-like (CML) proteins serve as primary Ca^{2+} sensors and regulate various cellular functions by modulating the activity of diverse target proteins (Cheval et al. 2013). Our assay of GO functional enrichment discovered that DEGs were enriched in functions like catalytic activity, binding, and transport activity, revealing that calcium regulates multiple cellular functions in *R. roxburghii* cells. Intriguingly, three pathways, namely, plant-pathogen interaction, MAPK signaling pathway, and plant hormone signal transduction, showed the highest percentage of DEGs in the KEGG pathway enrichment. Prior research has demonstrated that calcium signaling through Ca^{2+} influx in plant apoplast is a crucial stage for disease resistance proteins to function. A calmodulin-binding transcription factor links calcium signaling to antiviral RNAi defense in plants (Wang et al. 2021b). The ZAR1 protein has Ca^{2+}-selective channel activity and induces immunity and cell death (Bi et al. 2021). AtNLRs can create Ca^{2+}-permeable cation channels that modulate cytoplasmic Ca^{2+} levels and directly mediate cell death signals (Jacob et al. 2021). Intracellular immune receptors form atypical calcium-permeable cation channels in the PM and mediate a prolonged calcium influx, which overcomes the negative effects of pathogen effectors and enhances plant immune responses (Kim et al. 2022). Thus, we suggest that the mechanism of calcium uptake and translocation has a similar network to that of plant disease resistance.

4.2 Seven Gene Families Directly or Indirectly Regulate Calcium Transport Processes in R. roxburghii and Respond to Changes in Calcium Concentration

The treatment of sparying Ca^{2+} solution in vivo in grape triggers a tremendous number of DEGs associated with calcium transport, affecting the plant's calcium uptake (Yu et al. 2020). The transport and buffering processes of calcium depend on the participation of multiple ion channels and carrier proteins (Zhang et al. 2019). There were 25 genes involved in calcium uptake and transport process in this trial, covering seven gene families, including *ECA*, *ACA*, *GLR*, *CNGC*, *ZTP*, *MTP*, and *NRAMP*.

Table 1 Calcium absorption rate of *R. roxburghii* at different time points. *Note*: Values in the table are absorption rates ± standard errors, and * indicates that calcium absorption rate is significantly different at the 0.05 level

Time	Ca^{2+} uptake rate (μg g^{-1} h^{-1})
0 min	0.00 ± 0.00
5 min	1106.67 ± 58.10*
6 h	16.67 ± 4.09

There are two types of Ca^{2+}-pumping ATPase in plant cells, the ECAs and ACAs (Bonza and De Michelis 2011). The ACA is usually located on the plasma membrane, and it is highly selective, only transporting Ca^{2+} and promoting Ca^{2+} into the vacuole or the apoplast (Boursiac et al. 2010; Huda et al. 2013; Costa et al. 2017). ECA located in the endoplasmic reticulum (Dodd et al. 2010). Moeder et al. (2019)

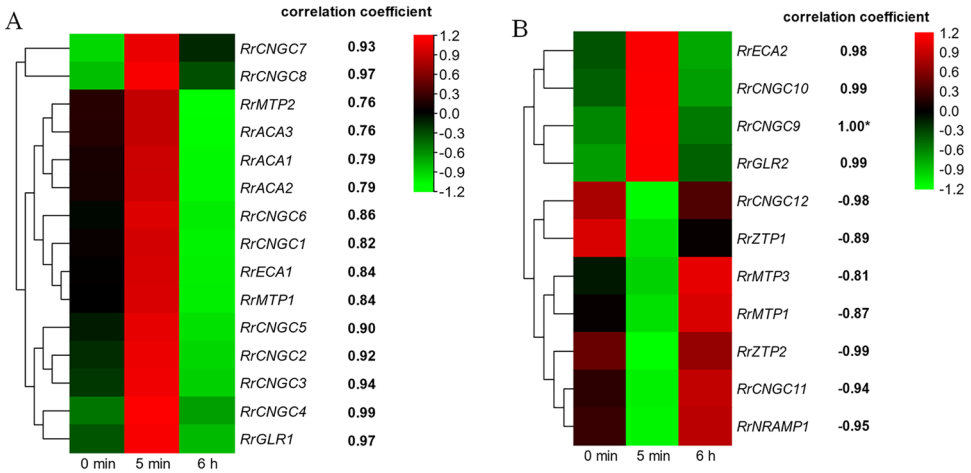

Fig. 4 Heat map of calcium absorption and transport-related gene expression in leaves (**A**) and sand roots (**B**) of *R. roxburghii*. Note: Values in the graph are correlation coefficients; *indicates that gene expression is significantly correlated with calcium uptake rate at the 0.05 level

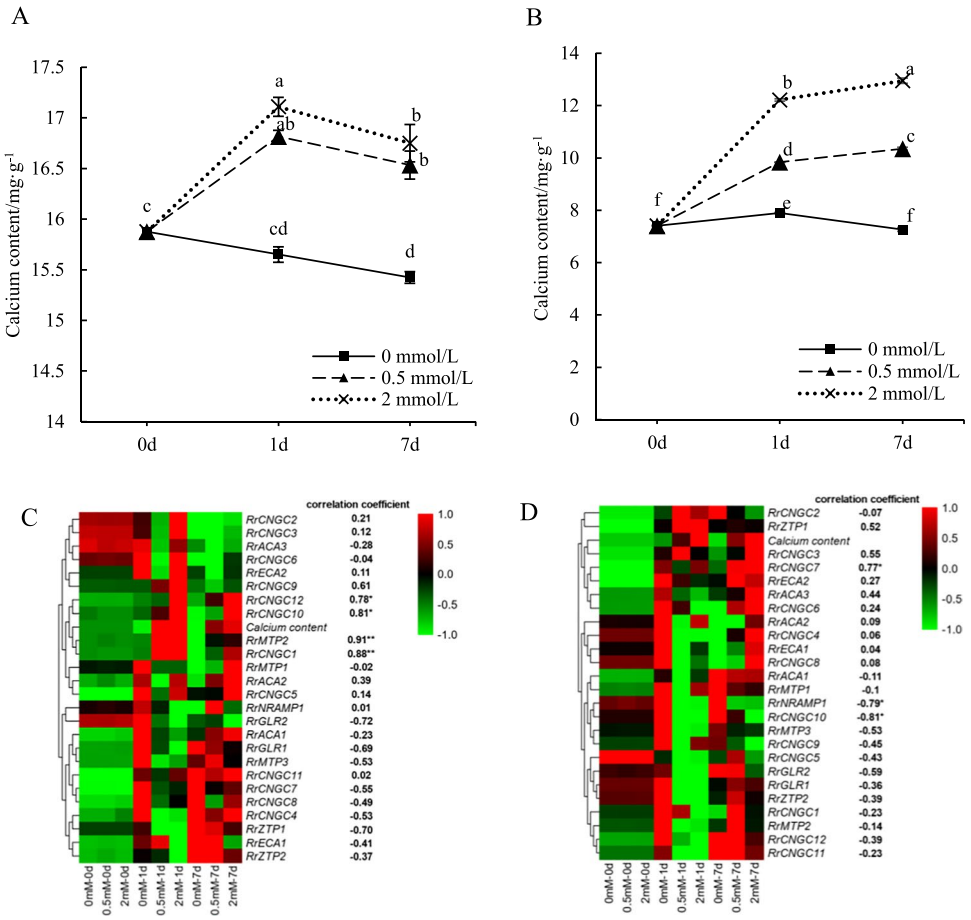

Fig. 5 Changes in calcium content of *R. roxburghii* leaves (**A**) and roots (**B**) under different calcium concentration treatments and changes in candidate gene expression in leaves (**C**) and roots (**D**). Note: Different letters in the figure indicate that the calcium content of different treatments has significant differences. The numbers in the heat map indicate the correlation coefficient between the expression levels of candidate genes and calcium content. *indicates that there is a significant correlation between gene expression and calcium content at the level of 0.05; **indicates that there is a very significant correlation at the level of 0.01

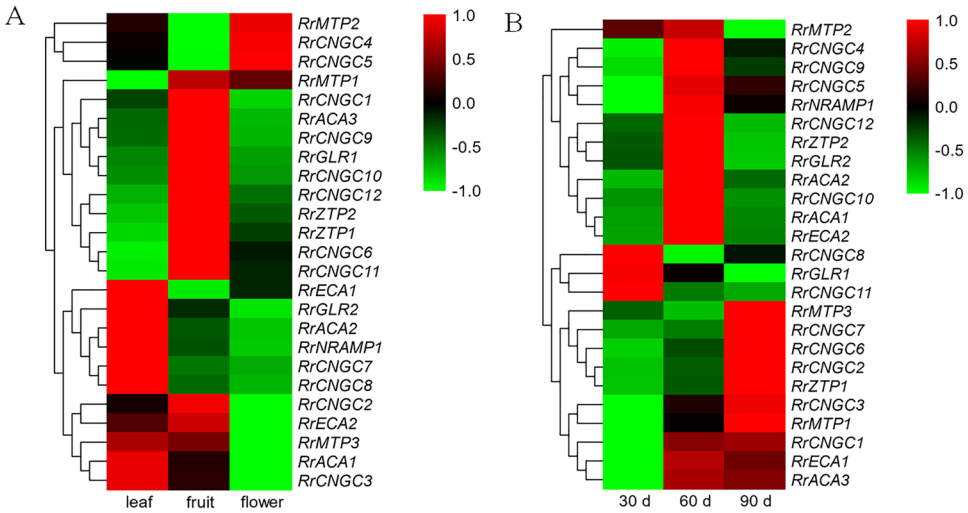

Fig. 6 Temporal and spatial expression characteristics of calcium absorption and transport related genes in *R. roxburghii*. Note: **A** The expression of candidate genes in leaves, petals, and 30-day fruits; **B** the expression of candidate genes in fruits of different development stages

suggested that two ligand-gated ion channel families, GLRs and CNGCs, play significant roles in immune responses. GLRs are located on the plasma membrane as non-selective Ca^{2+} channels that can mediate long-distance cytoplasmic Ca^{2+} signaling (Vincill et al. 2013; Suda and Toyota 2022). CNGCs are distributed across various organelle membranes, and it is usually activated by cAMP and cGMP to promote Ca^{2+} influx (Gobert et al. 2006; James and Zagotta 2018). Wang et al. (2021a) discovered that CNGC15 and the nitrate transceptor NRT1.1 as a molecular switch together to regulate calcium influx based on nitrate levels. This suggests that non-calcium transporter proteins could also influence calcium transport. Our study found a correlation between the expression of *RrMTPs*, *RrNRAMPs*, and *RrZTPs* families and the rate of calcium uptake. ZTPs are located in the endoplasmic reticulum membrane (Wang et al. 2010), increasing the zinc concentration in the cytosol (Baltaci and Yuce 2018). NRAMP is a type of bivalent metal transporter protein that transports ions like Fe^{2+}, Mn^{2+}, and Zn^{2+} from the apoplast or organelle to the cytosol (Nevo and Nelson 2006; Mani and Sankaranarayanan 2018), which located in the plasma membrane, endoplasmic reticulum membrane, and golgi membrane (Gao et al. 2018; Li et al. 2022). MTPs located in golgi, vacuole, and mitochondria can transfer Zn, Mn, and Fe into the organelle (Farthing et al. 2017; Gu et al. 2021; Migocka et al. 2018). Some MTPs located at the plasma membrane also contribute to the efflux of excess metal ions from plants and maintenance of ions homeostasis, like MTP10 (Ge et al. 2022a, b; Zhang et al. 2020; Migocka et al. 2015). Interestingly, in previous studies, *MTPs* and *NRAMPs* were mainly implicated in the transportation of Mg^{2+} and facilitated the transport of cations from the subsurface part to the aboveground part (He et al. 2021), and NRAMPs did not have the protein structure to transport Ca^{2+} (Ehrnstorfer et al. 2014). Ge et al. (2022a, b) found Ca^{2+} and Mg^{2+} have antagonistic effects, and MTP10 can maintain the homeostasis between Mg and Ca. We presume that NRAMPs, ZTPs, and MTPs mutually regulate each other, thereby coordinating ion homeostasis in *R. roxburghii*. However, further testing is required to support this theory.

The calcium uptake is a complex process, which requires different ion channels at various stages of uptake. Both leaves and roots serve as organs for plants to absorb nutrients. Unlike soil fertilization, nutrients sprayed on the leaf surface are mainly absorbed by crops through leaf cuticles and stomata (Niu et al. 2021). In this paper, only the mode of calcium uptake by the roots is discussed, and other modes need to be further explored. Based on previous literature, we predicted the functional pattern of each gene in a hypothetical *R. roxburghii* cell (Fig. 10). Ca^{2+} must cross the casparian strip and enter the cytoplasm through Ca^{2+} channels such as CNGCs and GLRs in the plasma membrane after contacting the epidermis of roots (Alcock et al. 2021). Subsequently, channel proteins such as MTPs, NRAMPs, ZTPs, and CNGCs play a dual role. On the one hand, they carry out long-distance signal transduction and promote upward transport of Ca^{2+} with the help of transpiration pull. On the other hand, they actively regulate ion homeostasis during calcium uptake. Finally, Ca^{2+} stored in the organelles of the leaf through ECAs and ACAs. Calcium absorption is affected by abiotic stress factors (Gong et al. 2020). The process correlates with calcium concentration in this experiment. We obtained different candidate genes in different concentrations of the culture solution, reflecting the fact that the uptake pattern changes depending on the calcium concentration. The reason for changes in transportation modes may be that calcium also plays roles as a second messenger coupling a wide range of extracellular stimuli with intracellular responses (Shao et al. 2008).

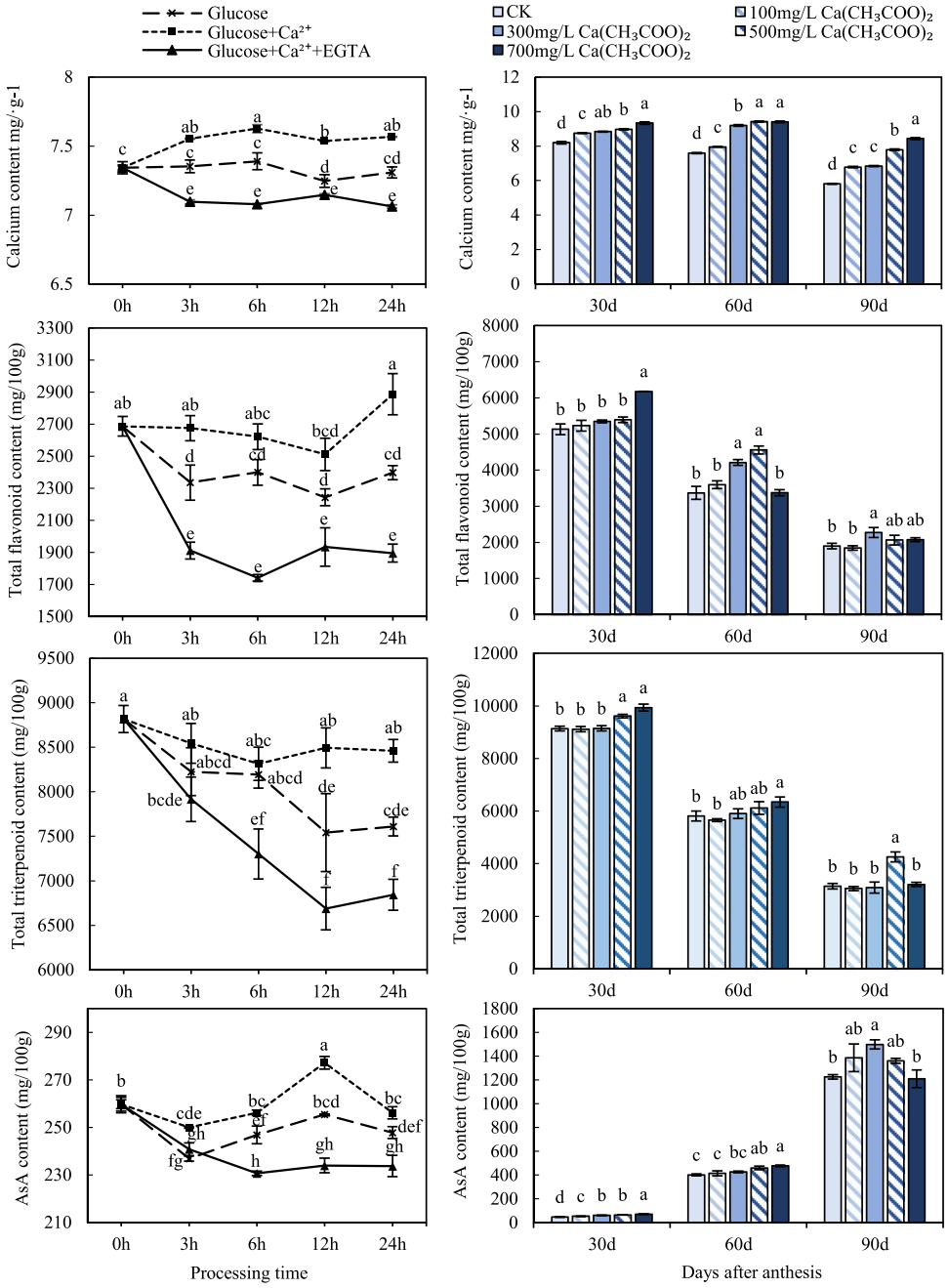

Fig. 7 Changes in calcium, AsA, total flavonoid, and total triterpenoid in fruits. Note: The left shows the results of Ca^{2+} soaking fruits in vitro, with glucose as the control; the right shows the results of Ca^{2+} spraying plant crown in vivo, with water as the control

4.3 The Expression of Transporter Proteins Is Spatiotemporally Specific and Involves the Synthesis of Bioactive Substances

The expression abundance of genes is not alike in different tissues. For example, *GLRs* preferentially expressed in root (Price et al. 2013). However, out of the 25 candidate genes, most show high expression levels in leaves and fruits (Fig. 6). Calcium oxalate crystals are found exclusively in the phloem of *R. roxburghii* leaves and stems, as well as in fruits under high-calcium conditions, but not in roots (Meng and Fan 2022). We hypothesize that the main role of transporter proteins in roots is to transport Ca^{2+} rather than store Ca^{2+}. As the fruit matured, the calcium content in fruit gradually decreased and differences in the expression pattern of ion channels appeared (Fig. 6). These results suggest that calcium absorption is also influenced by tissue and developmental stage.

Wang et al. (2016) discovered that the addition of Ca^{2+} increased the levels of gamma-aminobutyric acid, isoflavones, phenolics, and vitamins. When plants faced to $Ca(NO_3)_2$ stress, the levels of AsA and glutathione decreased significantly, along with the activities of antioxidant enzymes involved in the AsA-GSH cycle (Yuan et al. 2013). Similarly, we found that Ca^{2+} increased the accumulation of three active

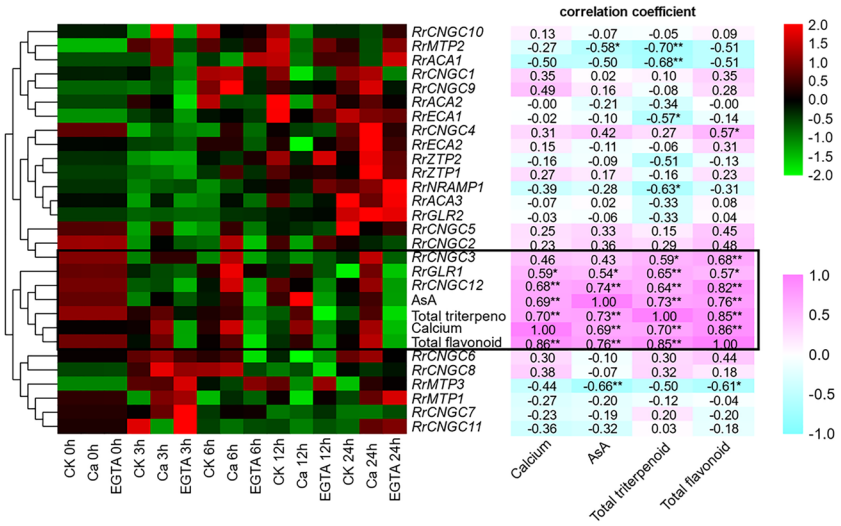

Fig. 8 Expression of candidate genes and its correlation analysis with calcium, AsA, total flavonoid, and total triterpenoid content after Ca^{2+} soaking fruits in vitro. Note: CK, 15 mmol L^{-1} glucose soaking treatment; Ca, 2 mmol L^{-1} $CaSO_4$ + 15 mmol L^{-1} glucose; EGTA, 2 mmol L^{-1} $CaSO_4$ + 15 mmol L^{-1} glucose + 5 mmol L^{-1} EGTA; 0 h, 3 h, 6 h, 12 h, and 24 h represent soaking time. The graph is divided into two parts: the left shows the heat map of gene expression, and the right shows the correlation analysis of gene expression with calcium, AsA, total flavonoid, and total triterpenoid content

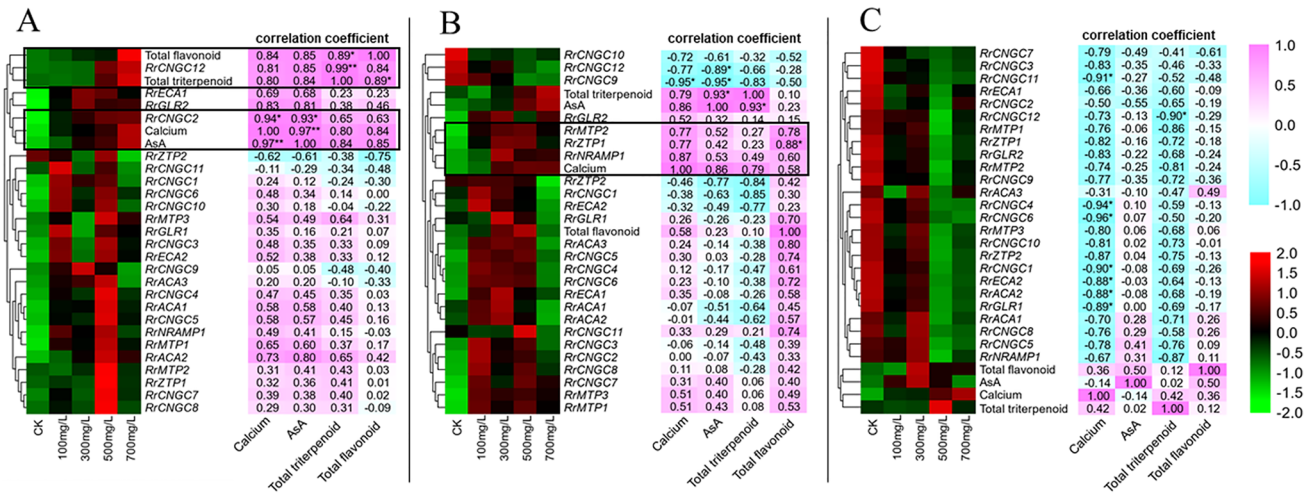

Fig. 9 Expression of candidate genes and its correlation analysis with calcium, AsA, total flavonoid, and total triterpenoid contents in fruits of **A** (30 days after anthesis), **B** (60 days after anthesis), and **C** (90 days after anthesis) after Ca^{2+} spraying plant crown in vivo. Note: CK, the water treatment, and the concentration in the figure is the concentration of $Ca(CH_3COO)_2$ used for spraying. Each graph is divided into two parts: the left shows the heat map of gene expression, and the right shows the correlation analysis of gene expression with calcium, AsA, total flavonoid, and total triterpenoid content

substances, including AsA, total triterpenoid, and total flavonoid in *R. roxburghii* fruits. Research shows that exogenous Ca^{2+} can alleviate SAR-induced oxidative damage to the cell membrane by enhancing antioxidative capacity (Liang et al. 2021). PMM interacts with CML10 to regulate AsA production in the presence of Ca^{2+} (Cho et al. 2016). Thus, Ca^{2+} is involved in the synthesis of active substances. Interestingly, as the fruit continued to develop, the Ca^{2+} content decreased, while the AsA content consistently increased. Exogenous AsA triggers a transient increase in $[Ca^{2+}]_{cyt}$ in *Arabidopsis* roots (Makavitskaya et al. 2018). Ca^{2+} may be regulated by feedback from substances such as AsA.

The expression of *RrCNGC12* and *RrGLR1* showed a significant and positive correlation with all three substances after Ca^{2+} soaking treatment (Fig. 8), indicating their potential role in the common pathway for these substances' synthesis.

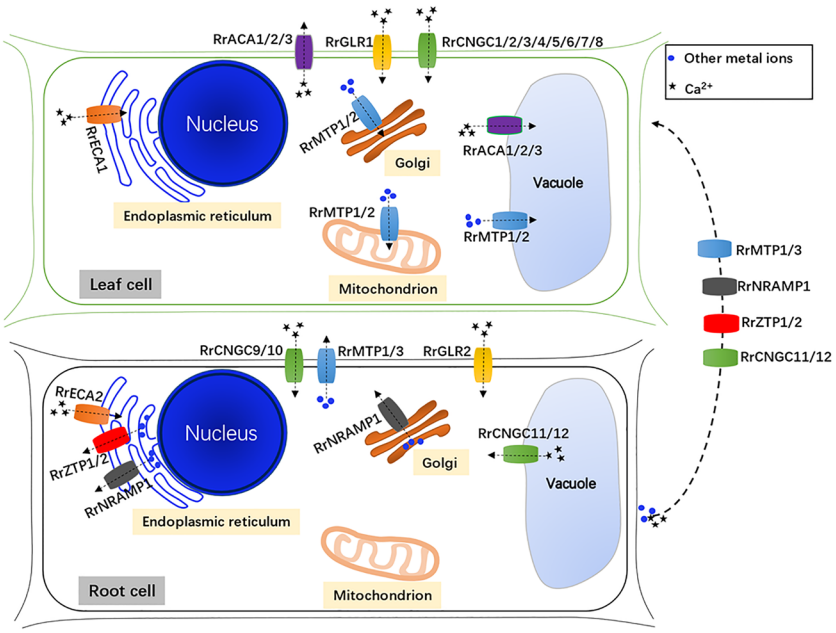

Fig. 10 Predicted functional patterns of candidate transporter proteins. Note: The figure shows the ion transport status of each candidate transporter protein in a hypothetical leaf cell and a hypothetical root cell in *R. roxburghii*. The arrow is the direction of ion transport

Additionally, the expression of *RrCNGC2* and AsA content in the fruits at 30 days after anthesis showed a highly significant and positive correlation, while the expression of *RrZTP1* was significantly and positively correlated with the total flavonoid content in the fruits at 60 days after anthesis (Fig. 9). The disparity in results between the two treatments could be ascribed to the intricacy of the calcium uptake process. The transport process entailed the movement of Ca^{2+} across various tissues in the Ca^{2+} spraying treatment. Previous research has demonstrated that exogenous Si boosts the tolerance of cucumber seedlings to cinnamic acid by upregulating the transcript levels of several enzyme genes involved in the AsA-GSH cycle pathway (Meng et al. 2021). Similarly, Ca^{2+} can transmit the secondary signals to downstream target enzymes and activate them to synthesize various secondary metabolites (Zhao et al. 2005). Based on these findings, we propose that *RrCNGC2/3/12*, *RrGLR1*, and *RrZTP1* in *R. roxburghii* fruits influence the accumulation of AsA, triterpenoid, and flavonoid from the protein level and transcriptional level by regulating the Ca^{2+} level. However, the specific mechanism needs further investigation.

5 Conclusion

In this research, 12,314 DEGs took park in the course of calcium uptake in *R. roxburghii*. We screened 15 and 11 genes involved in Ca^{2+} uptake in leaves and roots, respectively. Apart from the Ca^{2+} transport genes such as *CNGCs*, *ECAs*, *ACAs*, and *GLRs*, other metal ion transport genes such as *NRAMPs*, *ZTPs*, and *MTPs* are also involved in the Ca^{2+} uptake process and jointly regulate the ions homeostasis. The *CNGC* and *MTP* gene families are particularly instrumental in responding to changes of the exogenous calcium concentration. We have also observed that the exogenous calcium promotes AsA, flavonoid, and triterpenoid accumulation in fruits, and *RrCNGC12* play a critical role in this process. Overall, our findings preliminarily shed light on the molecular mechanisms of calcium uptake and the potential effects of Ca^{2+} on improving fruit quality formation.

Supplementary Information The online version contains supplementary material available at https://doi.org/10.1007/s42729-023-01579-8.

Author Contribution Huaming An: conceptualization, methodology, formal analysis, writing — review and editing, visualization, supervision, funding acquisition. Min Lu: resources, validation, investigation. Zhao Wang: software, formal analysis, investigation, visualization, writing — original draft.

Funding This work was supported by the Joint Fund of the National Natural Science Foundation of China and the Karst Science Research Center of Guizhou Province (No. U1812401) and the National Natural Science Foundation of China (grant no. 32260730).

Data Availability All sequencing data are available through the NCBI Sequence Read Archive under the accession number PRJNA993289.

Declarations

Competing Interests The authors declare no competing interests.

References

Ahmad P, Latef AAA, Abd Allah EF, Hashem A, Sarwat M, Anjum NA, Gucel S (2016) Calcium and potassium supplementation enhanced growth, osmolyte secondary metabolite production, and enzymatic antioxidant machinery in cadmium-exposed chickpea (Cicer arietinum L.). Front Plant Sci 7:513. https://doi.org/10.3389/fpls.2016.00513

Alcock TD, Thomas CL, Ó Lochlainn S, Pongrac P, Wilson M, Moore C, Reyt G, Vogel-Mikuš K, Kelemen M, Hayden R, Wilson L, Stephenson P, Østergaard L, Irwin JA, Hammond JP, King GJ, Salt DE, Graham NS, White PJ, Broadley MR (2021) Magnesium and calcium overaccumulate in the leaves of a *schengen3* mutant of *Brassica rapa*. Plant Physiol 186:1616–1631. https://doi.org/10.1093/plphys/kiab150

Apweiler R, Bairoch A, Wu CH, Barker WC, Boeckmann B, Ferro S, Gasteiger E, Huang H, Lopez R, Magrane M, Martin MJ, Natale DA, O'Donovan C, Redaschi N, Yeh LS (2004) UniProt: the Universal Protein knowledgebase. Nucleic Acids Res 32:D115-119. https://doi.org/10.1093/nar/gkh131

Ashburner M, Ball CA, Blake JA, Botstein D, Butler H, Cherry JM, Davis AP, Dolinski K, Dwight SS, Eppig JT, Harris MA, Hill DP, Issel-Tarver L, Kasarskis A, Lewis S, Matese JC, Richardson JE, Ringwald M, Rubin GM, Sherlock G (2000) Gene ontology: tool for the unification of biology. Gene Ontol Consortium Nat Genet 25:25–29. https://doi.org/10.1038/75556

Baltaci AK, Yuce K (2018) Zinc transporter proteins. Neurochem Res 43:517–530. https://doi.org/10.1007/s11064-017-2454-y

Bi GZ, Su M, Li N, Liang Y, Dang S, Xu JC, Hu MJ, Wang JZ, Zou MX, Deng YA, Li QY, Huang SJ, Li JJ, Chai JJ, He KM, Chen YH, Zhou JM (2021) The ZAR1 resistosome is a calcium-permeable channel triggering plant immune signaling. Cell 184:3528–3541. https://doi.org/10.1016/j.cell.2021.05.003

Bonza MC, De Michelis MI (2011) The plant Ca^{2+}-ATPase repertoire: biochemical features and physiological functions. Plant Biol 13:421–430. https://doi.org/10.1111/j.1438-8677.2010.00405.x

Boursiac Y, Lee SM, Romanowsky S, Blank R, Sladek C, Chung WS, Harper JF (2010) Disruption of the vacuolar calcium-ATPases in *Arabidopsis* results in the activation of a salicylic acid-dependent programmed cell death pathway. Plant Physiol 154:1158–1171. https://doi.org/10.1104/pp.110.159038

Bräutigam A, Gowik U (2010) What can next generation sequencing do for you? Next generation sequencing as a valuable tool in plant research. Plant Biol 12:831–841. https://doi.org/10.1111/j.1438-8677.2010.00373.x

Buchfink B, Xie C, Huson DH (2015) Fast and sensitive protein alignment using DIAMOND. Nat Methods 12:59–60. https://doi.org/10.1038/nmeth

Chen S, Zhou Y, Chen Y, Gu J (2018) fastp: an ultra-fast all-in-one FASTQ preprocessor. Bioinformatics 34:i884–i890. https://doi.org/10.1093/bioinformatics/bty560

Cheval C, Aldon D, Galaud JP, Ranty B (2013) Calcium/calmodulin-mediated regulation of plant immunity. Bba-Mol Cell Res 1833:1766–1771. https://doi.org/10.1016/j.bbamcr.2013.01.031

Cho KM, Nguyen HT, Kim SY, Shin JS, Cho DH, Hong SB, Shin JS, Ok SH (2016) CML10, a variant of calmodulin, modulates ascorbic acid synthesis. New Phytol 209:664–678. https://doi.org/10.1111/nph.13612

Costa A, Luoni L, Marrano CA, Hashimoto K, Koster P, Giacometti S, De Michelis MI, Kudla J, Bonza MC (2017) Ca^{2+}-dependent phosphor regulation of the plasma membrane Ca^{2+}-ATPase ACA8 modulates stimulus-induced calcium signatures. J Exp Bot 68:3215–3230. https://doi.org/10.1093/jxb/erx162

Demidchik V, Shabala S, Isayenkov S, Cuin TA, Pottosin I (2018) Calcium transport across plant membranes: mechanisms and functions. New Phytol 220:49–69. https://doi.org/10.1111/nph.15266

Deng YY, Li JQ, Wu SF, Zhu YP, Zhu YP, Chen YW, He FC (2006) Integrated nr database in protein annotation system and its localization. Comput Eng 32:71–74. https://doi.org/10.3969/j.issn.1000-3428.2006.05.026

Dodd AN, Kudla J, Sanders D (2010) The language of calcium signaling. Annu Rev Plant Biol 61:593–620. https://doi.org/10.1146/annurev-arplant-070109-104628

Ehrnstorfer IA, Geertsma ER, Pardon E, Steyaert J, Dutzler R (2014) Crystal structure of a SLC11 (NRAMP) transporter reveals the basis for transition-metal ion transport. Nat Struct Mol Biol 21:990–996. https://doi.org/10.1038/nsmb.2904

Fan WG, Yang HQ (2014) Response of root architecture, nutrients uptake and shoot growth of *Malus hupehensis* seedling to the shape of root zone. Chinese Agricultural Science 47:3907–3913. https://doi.org/10.3864/j.issn.0578-1752.2014.19.020

Farthing EC, Menguer PK, Fett JP, Williams LE (2017) OsMTP11 is localised at the Golgi and contributes to Mn tolerance. Sci Rep 7:15258. https://doi.org/10.1038/s41598-017-15324-6

Finn RD, Bateman A, Clements J, Coggill P, Eberhardt RY, Eddy SR, Heger A, Hetherington K, Holm L, Mistry J, Sonnhammer EL, Tate J, Punta M (2014) Pfam: the protein families database. Nucleic Acids Res 42:D222-230. https://doi.org/10.1093/nar/gkt1223

Gao QF, Gu LL, Wang HQ, Fei CF, Fang X, Hussain J, Sun SJ, Dong JY, Liu HT, Wang YF (2016) Cyclic nucleotide-gated channel 18 is an essential Ca^{2+} channel in pollen tube tips for pollen tube guidance to ovules in *Arabidopsis*. Proc Natl Acad Sci USA 113:3096–3101. https://doi.org/10.1073/pnas.1524629113

Gao H, Xie W, Yang C, Xu J, Li J, Wang H, Chen X, Huang CF (2018) NRAMP2, a trans-Golgi network-localized manganese transporter, is required for *Arabidopsis* root growth under manganese deficiency. New Phytol 217:179–193. https://doi.org/10.1111/nph.14783

Ge H, Shao Q, Chen J, Chen J, Li X, Tan Y, Lan W, Yang L, Wang Y (2022a) A metal tolerance protein, MTP10, is required for the calcium and magnesium homeostasis in *Arabidopsis*. Plant Signal Behav 17:2025322. https://doi.org/10.1080/15592324.2021.2025322

Ge H, Wang Y, Chen J, Zhang B, Chen R, Lan W, Luan S, Yang L (2022b) An *Arabidopsis* vasculature distributed metal tolerance protein facilitates xylem magnesium diffusion to shoots under high-magnesium environments. J Integr Plant Biol 64:166–182. https://doi.org/10.1111/jipb.13187

Gobert A, Park G, Amtmann A, Sanders D, Maathuis FJM (2006) *Arabidopsis thaliana* cyclic nucleotide gated channel 3 forms a non-selective ion transporter involved in germination and cation transport. J Exp Bot 57:791–800. https://doi.org/10.1093/jxb/erj064

Gong Z, Xiong L, Shi H, Yang S, Herrera-Estrella LR, Xu G, Chao DY, Li J, Wang PY, Qin F, Li J, Ding Y, Shi Y, Wang Y, Yang Y, Guo Y, Zhu JK (2020) Plant abiotic stress response and nutrient use efficiency. Sci China Life Sci 63:635–674. https://doi.org/10.1007/s11427-020-1683-x

Görlach BM, Sagervanshi A, Henningsen JN, Pitann B, Mühling KH (2021) Uptake, subcellular distribution, and translocation of foliar-applied phosphorus: short-term effects on ion relations in deficient young maize plants. Plant Physiol Bioch 166:677–688. https://doi.org/10.1016/j.plaphy.2021.06.028

Gu D, Zhou X, Ma Y, Xu E, Yu Y, Liu Y, Chen X, Zhang W (2021) Expression of a *Brassica napus* metal transport protein (BnMTP3) in *Arabidopsis thaliana* confers tolerance to Zn and Mn. Plant Sci 304:110754. https://doi.org/10.1016/j.plantsci.2020.110754

He KM, Chen YH, Zhou JM (2021) The ZAR1 resistosome is a calcium-permeable channel triggering plant immune signaling. Cell 184:3528–3541. https://doi.org/10.1016/j.cell.2021.05.003

Hirschi KD (2004) The calcium conundrum. Both versatile nutrient and specific signal. Plant Physiol 136:2438–2442. https://doi.org/10.1104/pp.104.046490

Huda KM, Banu MS, Tuteja R, Tuteja N (2013) Global calcium transducer P-type Ca^{2+}-ATPases open new avenues for agriculture by regulating stress signalling. J Exp Bot 64:3099–3109. https://doi.org/10.1093/jxb/ert182

Jacob P, Kim NH, Wu FH, El Kasmr F, Chi Y, Walton WG, Furzer OJ, Lietzan AD, Sunil S, Kempthorn K, Redinbo MR, Pei ZM, Wan L, Dangl JL (2021) Plant "helper" immune receptors are Ca^{2+}-permeable nonselective cation channels. Science 373:420–425. https://doi.org/10.1126/science.abg7917

James ZM, Zagotta WN (2018) Structural insights into the mechanisms of CNBD channel function. J Gen Physiol 150:225–244. https://doi.org/10.1085/jgp.201711898

Juric S, Stracenski KS, Krol-Kilinska Z, Zutic I, Uher SF, Dermic E, Topolovec-Pintaric S, Vincekovic M (2020) The enhancement of plant secondary metabolites content in Lactuca sativa L. by encapsulated bioactive agents. Sci Rep 10:3737. https://doi.org/10.1038/s41598-020-60690-3

Kanehisa M, Goto S, Kawashima S, Okuno Y, Hattori M (2004) The KEGG resource for deciphering the genome. Nucleic Acids Res 32:D277–D280. https://doi.org/10.1093/nar/gkh063

Kanehisa M, Araki M, Goto S, Hattori M, Hirakawa M, Itoh M, Katayama T, Kawashima S, Okuda S, Tokimatsu T, Yamanishi Y (2008) KEGG for linking genomes to life and the environment. Nucleic Acids Res 36:D480-484. https://doi.org/10.1093/nar/gkm882

Kim D, Langmead B, Salzberg SL (2015) HISAT: a fast spliced aligner with low memory requirements. Nat Methods 12:357–360. https://doi.org/10.1038/nmeth.3317

Kim NH, Jacob P, Dangl JL (2022) Con-Ca^{2+}-tenating plant immune responses via calcium-permeable cation channels. New Phytol 234:813–818. https://doi.org/10.1111/nph.18044

Koonin EV, Fedorova ND, Jackson JD, Jacobs AR, Krylov DM, Makarova KS, Mazumder R, Mekhedov SL, Nikolskaya AN, Rao BS, Rogozin IB, Smirnov S, Sorokin AV, Sverdlov AV, Vasudevan S, Wolf YI, Yin JJ, Natale DA (2004) A comprehensive evolutionary classification of proteins encoded in complete eukaryotic genomes. Genome Biol 5:R7. https://doi.org/10.1186/gb-2004-5-2-r7

Lecourieux D, Ranjeva R, Pugin A (2006) Calcium in plant defence-signalling pathways. New Phytol 171:249–269. https://doi.org/10.1111/j.1469-8137.2006.01777.x

Li L, Zhu Z, Liao Y, Yang C, Fan N, Zhang J, Yamaji N, Dirick L, Ma JF, Curie C, Huang CF (2022) NRAMP6 and NRAMP1 cooperatively regulate root growth and manganese translocation under manganese deficiency in *Arabidopsis*. Plant J 110:1564–1577. https://doi.org/10.1111/tpj.15754

Li LL, An HM (2016) Effects of Ca^{2+} and Cu^{2+} on the expression of genes related to AsA metabolism in *Rosa roxburghii*. Fruits. J Hortic 43:1377–1382. http://doi.org/10.16420/j.issn.0513-353x.2016-0013

Liang C, Zhang Y, Ren X (2021) Calcium regulates antioxidative isozyme activity for enhancing rice adaption to acid rain stress. Plant Sci 306:110876. https://doi.org/10.1016/j.plantsci.2021.110876

Liu JY, Niu YF, Zhang JJ, Zhou YQ, Ma Z, Huang X (2018) Ca^{2+} channels and Ca^{2+} signals involved in abiotic stress responses in plant cells: recent advances. Plant Cell Tiss Org 132:413–424. https://doi.org/10.1007/s11240-017-1350-0

Love MI, Huber W, Anders S (2014) Moderated estimation of fold change and dispersion for RNA-seq data with DESeq2. Genome Biol 15:550. https://doi.org/10.1186/s13059-014-0550-8

Luo C, Fan WG, Liu JP, An HM (2004) Effects of different treatments on fruit development of *Rosa roxburghii* Tratt. J Guizhou Normal Univ (Natl Sci Ed) 4:7–11. https://doi.org/10.3969/j.issn.1004-5570.2004.04.002

Makavitskaya M, Svistunenko D, Navaselsky I, Hryvusevich P, Mackievic V, Rabadanova C, Tyutereva E, Samokhina V, Straltsova D, Sokolik A, Voitsekhovskaja O, Demidchik V (2018) Novel roles of ascorbate in plants: induction of cytosolic Ca^{2+} signals and efflux from cells via anion channels. J Exp Bot 69:3477–3489. https://doi.org/10.1093/jxb/ery056

Mani A, Sankaranarayanan K (2018) In silico analysis of natural resistance-associated macrophage protein (NRAMP) family of transporters in rice. Protein J 37:237–247. https://doi.org/10.1007/s10930-018-9773-y

Martins V, Unlubayir M, Teixeira A, Geros H, Lanoue A (2021) Calcium and methyl jasmonate cross-talk in the secondary metabolism of grape cells. Plant Physiol Bioch 165:228–238. https://doi.org/10.1016/j.plaphy.2021.05.034

Meng QJ, Fan WG (2022) Calcium-tolerance type and adaptability to high-calcium habitats of *Rosa roxburghii*. Chin J Plant Ecol 46:1562–1572. https://doi.org/10.17521/cjpe.2022.0172

Meng X, Luo SL, Dawuda MM, Gao XQ, Wang SY, Xie JM, Tang ZQ, Liu ZC, Wu Y, Jin L, Lyu J, Yu JH (2021) Exogenous silicon enhances the systemic defense of cucumber leaves and roots against CA-induced autotoxicity stress by regulating the ascorbate-glutathione cycle and photosystem II. Ecotox Environ Safe 227:112879. https://doi.org/10.1016/j.ecoenv.2021.112879

Michailidis M, Karagiannis E, Tanou G, Sarrou E, Stavridou E, Ganopoulos I, Karamanoli K, Madesis P, Martens S, Molassiotis A (2019) An integrated metabolomic and gene expression analysis identifies heat and calcium metabolic networks underlying postharvest sweet cherry fruit senescence. Planta 250:2009–2022. https://doi.org/10.1007/s00425-019-03272-6

Migocka M, Papierniak A, Kosieradzka A, Posyniak E, Maciaszczyk-Dziubinska E, Biskup R, Garbiec A, Marchewka T (2015) Cucumber metal tolerance protein CsMTP9 is a plasma membrane H^+-coupled antiporter involved in the Mn^{2+} and Cd^{2+} efflux from root cells. Plant J 84:1045–1058. https://doi.org/10.1111/tpj.13056

Migocka M, Małas K, Maciaszczyk-Dziubinska E, Posyniak E, Migdal I, Szczech P (2018) Cucumber Golgi protein CsMTP5 forms a Zn-transporting heterodimer with high molecular mass protein CsMTP12. Plant Sci 277:196–206. https://doi.org/10.1016/j.plantsci.2018.09.011

Moeder W, Phan V, Yoshioka K (2019) Ca^{2+} to the rescue - Ca^{2+} channels and signaling in plant immunity. Plant Sci 279:19–26. https://doi.org/10.1016/j.plantsci.2018.04.012

Nevo Y, Nelson N (2006) The NRAMP family of metal-ion transporters. Bba-Mol Cell Res 1763:609–620. https://doi.org/10.1016/j.bbamcr.2006.05.007

Niu JH, Liu C, Huang ML, Liu KZ, Yan DY (2021) Effects of foliar fertilization: a review of current status and future perspectives. J Soil Sci Plant Nut 21:104–118. https://doi.org/10.1007/s42729-020-00346-3

Ojo O, Mphahlele MP, Oladeji OS, Mmutlane EM, Ndinteh DT (2022) From wandering weeds to pharmacy: an insight into traditional uses, phytochemicals and pharmacology of genus *Chromolaena* (Asteraceae). J Ethnopharmacol 291:115155. https://doi.org/10.1016/j.jep.2022.115155

Pertea M, Pertea GM, Antonescu CM, Chang TC, Mendell JT, Salzberg SL (2015) StringTie enables improved reconstruction of a transcriptome from RNA-seq reads. Nat Biotechnol 33:290–295. https://doi.org/10.1038/nbt.3122

Price MB, Kong D, Okumoto S (2013) Inter-subunit interactions between glutamate-like receptors in *Arabidopsis*. Plant Signal Behav 8:e27034. https://doi.org/10.4161/psb.27034

Sanders D, Brownlee C, Harper JF (1999) Communicating with calcium. Plant Cell 11:691–706. https://doi.org/10.1105/tpc.11.4.691

Sanders D, Pelloux J, Brownlee C, Harper JF (2002) Calcium at the crossroads of signalling. Plant Cell. 14:S401–S417. https://doi.org/10.1105/tpc.002899

Shao HB, Song WY, Chu LY (2008) Advances of calcium signals involved in plant anti-drought. Cr Biol 331:587–596. https://doi.org/10.1016/j.crvi.2008.03.012

Shi QW, Song QB, Wang HX, Bai CM, Wu D, Dong QP, Cheng X, Han XR, Liu YF (2017) Research progress of plant calcium nutrition

and calcium/cold signal interaction. ABSR BBE 2017 4:99–102. https://doi.org/10.2991/bbe-17.2017.16

Suda H, Toyota M (2022) Integration of long-range signals in plants: a model for wound-induced Ca^{2+}, electrical, ROS, and glutamate waves. Curr Opin Plant Biol 69:102270. https://doi.org/10.1016/j.pbi.2022.102270

Tang RJ, Luan S (2017) Regulation of calcium and magnesium homeostasis in plants: from transporters to signaling network. Curr Opin Plant Biol 39:97–105. https://doi.org/10.1016/j.pbi.2017.06.009

Tatusov RL, Galperin MY, Natale DA, Koonin EV (2000) The COG database: a tool for genome-scale analysis of protein functions and evolution. Nucleic Acids Res 28:33–36. https://doi.org/10.1093/nar/28.1.33

Vafadar F, Amooaghaie R, Ehsanzadeh P, Ghanadian M, Talebi M, Ghanati F (2020) Melatonin and calcium modulate the production of rosmarinic acid, luteolin, and apigenin in *Dracocephalum kotschyi* under salinity stress. Phytochemistry 177:112422. https://doi.org/10.1016/j.phytochem.2020.112422

Véry AA, Davies JM (2000) Hyperpolarization-activated calcium channels at the tip of *Arabidopsis* root hairs. Proc Natl Acad Sci USA 97:9801–9806. https://doi.org/10.1073/pnas.160250397

Vincill ED, Clarin AE, Molenda JN, Spalding EP (2013) Interacting glutamate receptor-like proteins in phloem regulate lateral root initiation in *Arabidopsis*. Plant Cell 25:1304–1313. https://doi.org/10.1105/tpc.113.110668

Wang M, Xu Q, Yu J, Yuan M (2010) The putative *Arabidopsis* zinc transporter ZTP29 is involved in the response to salt stress. Plant Mol Biol 73:467–479. https://doi.org/10.1007/s11103-010-9633-4

Wang XK, Yang RQ, Zhou YL, Gu ZX (2016) A comparative transcriptome and proteomics analysis reveals the positive effect of supplementary Ca^{2+} on soybean sprout yield and nutritional qualities. J Proteomics 143:161–172. https://doi.org/10.1016/j.jprot.2016.04.020

Wang XH, Feng CX, Tian LL, Hou CC, Tian W, Hu B, Zhang Q, Ren ZJ, Niu Q, Song JL, Kong DD, Liu LY, He YK, Ma LG, Chu CC, Luan S, Li LG (2021a) A transceptor-channel complex couples nitrate sensing to calcium signaling in *Arabidopsis*. Mol Plant 14:774–786. https://doi.org/10.1016/j.molp.2021.02.005

Wang Y, Gong Q, Wu Y, Huang F, Ismayil A, Zhang D, Li H, Gu H, Ludman M, Fátyol K, Qi Y, Yoshioka K, Hanley-Bowdoin L, Hong Y, Liu Y (2021b) A calmodulin-binding transcription factor links calcium signaling to antiviral RNAi defense in plants. Cell Host Microbe 29:1393–1406. https://doi.org/10.1016/j.chom.2021.07.003

Wang Z, Wang LH, Li JX, Yang W, Ci JB, Ren XJ, Wang W, Wang YB, Jiang LY, Yang WG (2022) Identification and expression analysis revealed drought stress-responsive Calmodulin and Calmodulin-like genes in maize. J Plant Interact 17:450–461. https://doi.org/10.1080/17429145.2022.2047235

Wang LL, An HM (2013) Optimization of a method for the determination of vitamin C in *Rosa roxburghii* fruits by HPLC. Modern Food Science and Technology 29: 397–400. https://doi.org/10.13982/j.mfst.1673-9078.2013.02.009

Yang HR, Fan WG (2022) Effects of different calcium supply levels on growth, mineral element absorption and related physiological and biochemical characteristics of *Rosa roxburghii* seedlings. J Fruit Sci 39:1891–1902. https://doi.org/10.13925/j.cnki.gsxb.20220101

Yang JS, Li WL, Xing C, Xing GN, Guo YX, Yuan HL (2022) Ca^{2+} participates in the regulation of microalgae triacylglycerol metabolism under heat stress. Environ Res 208:112696. https://doi.org/10.1016/j.envres.2022.112696

Young MD, Wakefield MJ, Smyth GK, Oshlack A (2010) Gene ontology analysis for RNA-seq: accounting for selection bias. Genome Biol 11:R14. https://doi.org/10.1186/gb-2010-11-2-r14

Yu J, Zhu MT, Wang MJ, Xu YS, Chen WT, Yang GS (2020) Transcriptome analysis of calcium-induced accumulation of anthocyanins in grape skin. Sci Hortic-Amsterdam 260:108871. https://doi.org/10.1016/j.scienta.2019.108871

Yuan LY, Du J, Yuan YH, Shu S, Sun J, Guo SR (2013) Effects of 24-epibrassinolide on ascorbate-glutathione cycle and polyamine levels in cucumber roots under $Ca(NO_3)_2$ stress. Acta Physiol Plant 35:253–262. https://doi.org/10.1007/s11738-012-1071-2

Zhang X, Yang M, An HM, Huang W, Liu W (2012) Effects of exogenous divalent cations Ca^{2+}, Mg^{2+}, and Cu^{2+} and acriflavine on ascorbate biosynthesis in *Rosa roxburghii* fruits. Chin Agric Sci 45:1144–1149. https://doi.org/10.3864/j.issn.0578-1752.2012.06.012

Zhang XM, Liu LX, Su ZM, Shen ZJ, Gao GF, Yi Y, Zheng HL (2019) Transcriptome analysis of *Medicago lupulina* seedlings leaves treated by high calcium provides insights into calcium oxalate formation. Plant Soil 444:299–314. https://doi.org/10.1007/s11104-019-04283-8

Zhang X, Li Q, Xu W, Zhao H, Guo F, Wang P, Wang Y, Ni D, Wang M, Wei C (2020) Identification of MTP gene family in tea plant (Camellia sinensis L.) and characterization of CsMTP8.2 in manganese toxicity. Ecotox Environ Safe 202:110904. https://doi.org/10.1016/j.ecoenv.2020.110904

Zhao J, Davis LC, Verpoorte R (2005) Elicitor signal transduction leading to production of plant secondary metabolites. Biotechnol Adv 23:283–333. https://doi.org/10.1016/j.biotechadv.2005.01.003